Structure and luminescence of sol-gel synthesized anatase nanoparticles

2010 J. Phys.: Conf. Ser. 209 012039

(http://iopscience.iop.org/1742-6596/209/1/012039)

Journal of Physics: Conference Series **209** (2010) 012039 doi:10.1088/1742-6596/209/1/012039

Structure and luminescence of sol-gel synthesized anatase nanoparticles

U Hörmann[1], U Kaiser[1], M Albrecht[2], J Geserick[3] and N Hüsing[3]

[1] Ulm University, Electron Microscopy Group of Materials Science, Albert-Einstein-Allee 11, 89081 Ulm, Germany
[2] Leibniz Institute for Crystal Growth, Max-Born-Str. 6, 12489 Berlin, Germany
[3] Ulm University, Institute of Inorganic Chemistry I, Albert-Einstein-Allee 11, 89081 Ulm, Germany

E-mail: ute.hoermann@uni-ulm.de

Abstract. Two samples of mesoporous anatase nanoparticles, prepared by the sol-gel method, were characterised by Cs-corrected high resolution transmission electron microscopy (HRTEM), X-ray powder diffraction (XRD) and Raman spectroscopy. Statistical evaluation of TEM data showed an average diameter of these crystallites of 8.8 nm and 11.1 nm, respectively. Optical spectroscopy by cathodoluminescence (CL) in a scanning electron microscope (SEM) showed free exciton transitions related to the direct and the indirect band gap of anatase TiO_2. From the analysis of the excited states of the free excitons an exciton binding energy of 10 meV and a Bohr radius of 2.35 nm is obtained. The small Bohr radius could explain the absence of quantum confinement in the particles presented in this study.

1. Introduction

Anatase is a wide band gap semiconductor with indirect band gap [1]. The band gap of bulk anatase was calculated by Wunderlich [2] to 3.20 eV, which is in accordance with experimental results.

Applications of mesostructured nanocrystalline titania are based on photoexcitation. In particular, titania is an important material in photo catalysis [3] due to its high catalytic activity. Other applications using photon excitations are the Grätzel type solar cell [4] and electrochromic devices [5].

It is therefore of great interest to get access to basic materials properties, such as the Bohr radius, effective masses and band structure to understand the size dependence of the electronic properties. While size dependence has been extensively studied and measured in terms of size dependent Raman shifts or photo luminescence transition lines [1,6], the existence of a quantum confinement effect in anatase and rutile nanoparticles is still under debate, e.g. questioned by Monticone et al. [7] who performed absorption measurements of anatase TiO_2 with sizes ranging from 2-8nm and found no indications for the existence of quantum confinement at all. These authors explained their findings by a size dependence of the effective hole mass in this material system.

2. Experiment

The anatase nanoparticles were synthesised in a sol-gel process at room temperature at pH=2. The sample denoted SDS was prepared from ethylene glycol modified titanate (EGMT) in the presence of

the surfactant sodium dodecyl sulphate (SDS) in a molar ratio of SDS:Ti = 0.2:1. For the sample denoted as Brij56 glycol modified titanate (GMT) was converted in the presence of the surfactant Brij56 in a molar ratio of Brij56:Ti=0.03:1. After drying the samples they were calcined for 4 h at 400 °C in air in order to remove the surfactant.

Nitrogen sorption measurements were performed on a NOVA 4000e and Autosorp MP1 instrument (Quantachrome). The surface area was calculated according to Brunauer, Emmett and Teller (BET) in the p/p_0 range of 0.05-0.3 and the pore size distribution was determined according to Barrett, Joyner and Halenda (BJH) from the desorption branch of the isotherms.

XRD measurements were performed by using Cu-K_α radiation ($\lambda = 0.154$ nm) on a PANalytical MPD PRO diffractometer.

For the TEM sample preparation the powders were dispersed in ethanol and 5 minutes treated in an ultrasonic bath. Afterwards the dispersion was dripped onto a holey carbon film coated copper grid. The samples were structurally characterised by Cs-corrected high resolution transmission electron microscopy using a FEI Titan 80-300 operated at 300 kV.

Raman measurements were carried out on a Jobin-Yvon LabRam using a 630 nm laser for excitation. Cathodoluminescence spectroscopy has been performed using a Zeiss DSM microscope with a Gatan MonoCL3 cathodoluminescence system attached. Light was dispersed by a 2400 l/mm grating blazed at 300 nm. A Peltier cooled charge coupled device camera was used for detection.

3. Results and Discussion

3.1 HRTEM

The HRTM images show that in both samples the anatase is nanocrystalline and mesoporous. The nanoparticles in both samples are either facetted or exhibit an irregular roundish shape. Particles with bad crystallinity or amorphous particles, not shown here, were observed more often in the Brij56 sample than in SDS. However, it has to be considered that the anatase is unstable against irradiation under the electron beam. Thus, no quantification can be made on the relative amount of amorphous anatase in the samples. Defects are observed in both samples, e.g. twins, see figure 1.

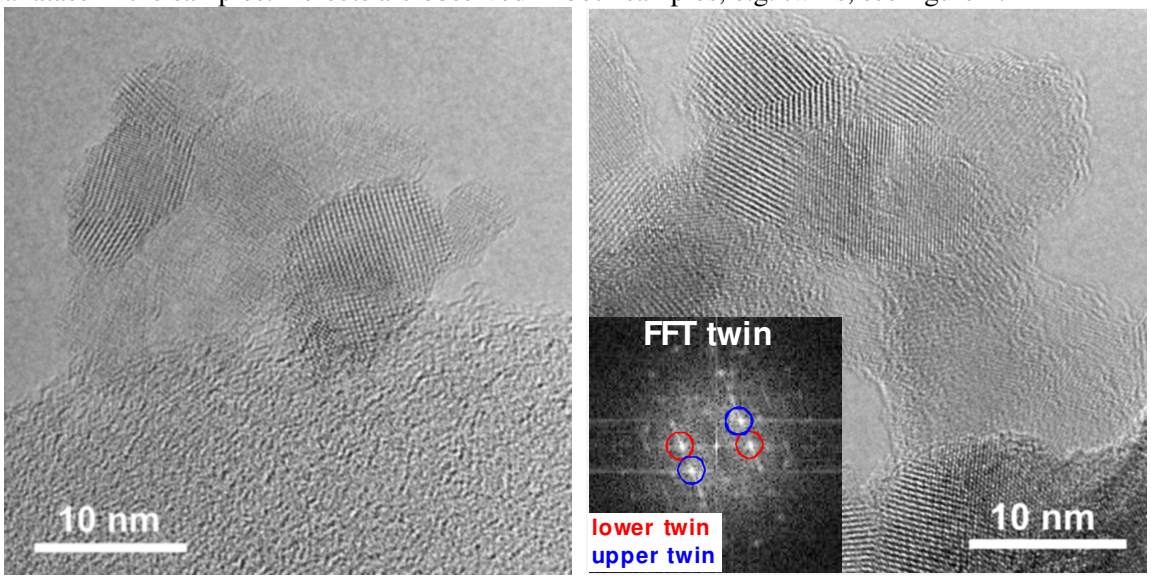

Figure 1. Cs-corrected HRTEM images of the anatase nanoparticles. Left: the SDS sample. Right: the Brij56 sample with crystalline nanoparticles and a twin. Inset: power spectrum.

Particle statistics was performed on both samples. 495 particles were measured on SDS and lead to an average particle size of 8.8±2.7 nm in diameter, ranging from 3 to 19 nm. On the Brij56 sample 485 particles were evaluated, resulting in an average diameter of 11.1±3.2 nm ranging from 5 to 23 nm.

3.2 X-Ray Powder Diffractometry

Both samples were found to consist of pure anatase, see figure 2. The particle sizes were determined from the FWHM of the {101} reflection, using the Scherrer equation with a form factor of K=0.9. The resulting particle diameters were 7.0 nm for the SDS sample and 6.2 nm for the Brij56 sample. These values are smaller than the diameters determined from the TEM micrographs. A possible explanation for this discrepancy may be the following [8]: (i) in very small particles the lattice constant depends on the crystallite size. This variation causes peak broadening. (ii) twin domains contribute twice, independently, to the spectrum while for the TEM analysis a twinned particle was counted only once. (iii) oxygen saturation in the surface area causes peak broadening. In all these cases peak broadening leads to an underestimate of the particle diameter from XRD. Nevertheless, the quantitative effect for these powders is a matter for further investigation.

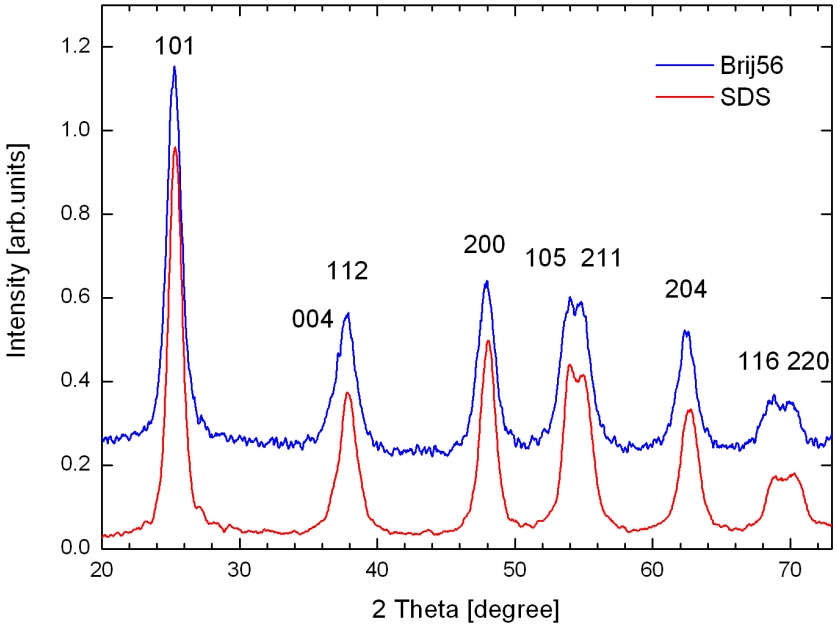

Figure 2. X-ray diffraction pattern of both samples with anatase reflections indicated.

3.3 Raman Spectroscopy

The Raman measurements show the phonon excitations for anatase. The crystallite size can be determined from the peak positions and from the full widths at half maximum (FWHM) of the E_g peak, see figure 3 [9]. The E_g peak of SDS has the maximum at 147.4±0.2 cm^{-1}. The maximum in the Brij56 sample was found at 145.2±0.1 cm^{-1}. The resulting particle diameters are 8 nm for SDS and 18 nm for Brij56. The FWHM measures 16.3±0.5 cm^{-1} for SDS and 12.4±0.1 cm^{-1} for Brij56. This leads to 6 nm particle diameter in SDS and 8 nm in Brij56. Again, in accordance with the TEM measurements the nanoparticles are larger in the Brij56 sample.

3.4 Nitrogen sorption

From the nitrogen sorption the BET surface area was determined to 184 m^2/g for the SDS sample and 140 m^2/g for the Brij56 sample. The pore diameter was determined to 4.9 nm for SDS and 6.9 nm for Brij56. The lower surface area and larger pore size for the Brij56 are in agreement with the results from TEM particle statistics and Raman spectroscopy, demonstrating larger particle size in Brij56.

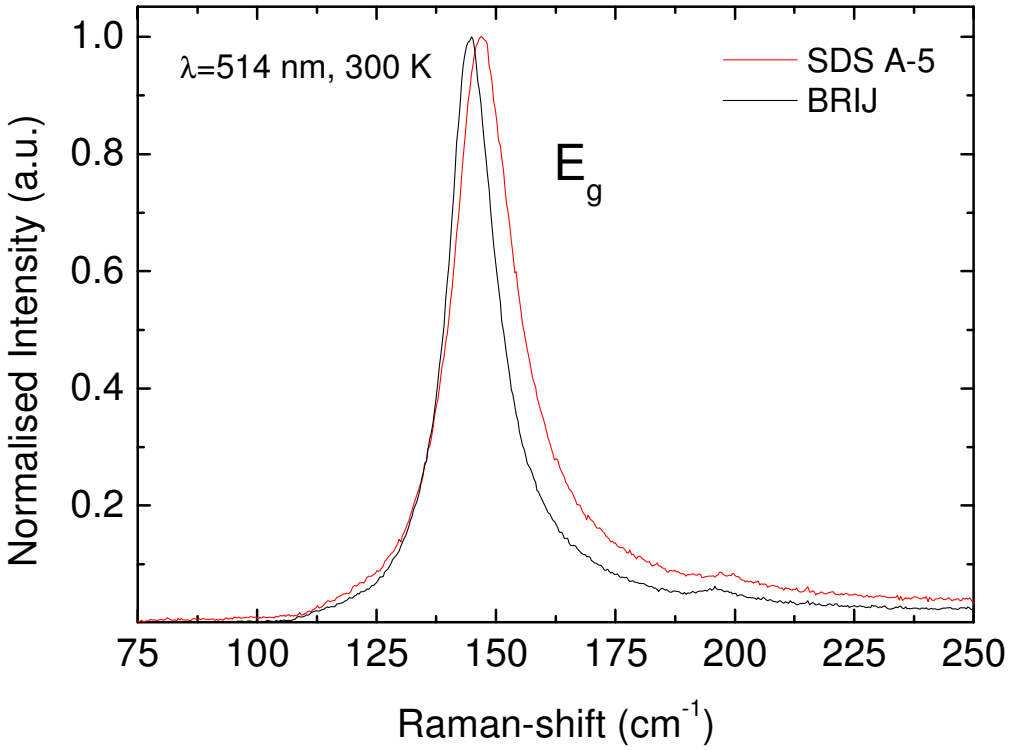

Figure 3. Raman spectrum of both samples. Shift of the E_g peak is due to phonon confinement.

3.5 Scanning electron microscopy cathodoluminescence investigation

Cathodoluminescence (CL) measurements have been performed on both samples. Optical transitions of the samples were independent of the average crystal size of the analysed samples; spatially integrated spectra at 7 K are dominated by a broad luminescence band centred at 2.26 eV. This broad band has been reported to appear in anatase phase TiO_2 single crystals, epitaxial layers and nano-crystals and has been attributed to self-trapped excitons at the TiO_6 octahedron [10]. Site selective spectra taken with a focused electron beam revealed transitions at 3.35 eV, with a line width of about 4 meV. Spectra taken at different sites indicated spatial anti-correlation of areas showing broad band luminescence at 2.26 eV and of those showing sharp UV transitions. Figure 4 shows a typical CL spectrum of the sharp transitions at higher energy resolution. At the high energy site two main peaks at 3.3962 and 3.3535 eV are dominating the spectrum. Both lines can be fitted by Lorentzian curves. The lines are separated by 42 meV. The higher energy transition has an intensity that is about 1% of that at lower energies. Temperature dependent measurements show a shift to lower energies according to that of the band gap of anatase TiO_2 reported by Tang [11]. Beside the main transition a number of phonon replica are observed. While the lower energy line at ~3.35eV has exclusively replica that correspond to the B_{1g} mode, the higher energy transition at ~3.40eV has additional replica that are higher in intensity than the main peak. The latter is characteristic for the zero phonon line and its phonon replica of indirect transitions in semiconductors.

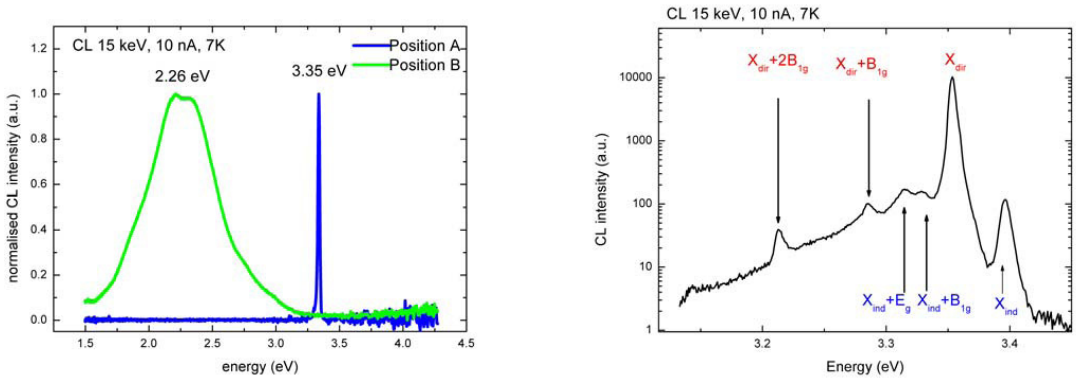

Figure 4. CL spectra typical for both samples. Left: overview at different locations. Right: high resolution spectrum of excitonic transitions.

Tang et al. [11] report on an indirect and direct gap that was found at 3.46 and 3.42 eV, respectively from absorption measurements in anatase single crystals. From the energy separation of the optical transitions, their intensity relation and their specific phonon replica it is tempting to assign the transitions found in our anatase nanocrystals to free excitonic transitions at the direct and indirect gap of anatase TiO_2. To confirm this we may in the following focus on the direct transition and its phonon replica. As can be seen in Figure 4 the 1- and 2- phonon replica have an asymmetric shape, with a steep edge at the low energy side and a high energy wing. This shape, if retained after background subtraction, could be characteristic for free excitons and due to the kinetic energy of the excitons that is described by a Maxwell distribution. Further support for the hypothesis of free excitons comes from the almost linear increase of the FWHM of the luminescence peaks with increasing temperature. The transition at 3.3535 eV in Figure 4 shows a high energy shoulder. A spectrum of that transition at higher resolution is shown in Figure 5. A second peak is revealed with an energy separation of 7.48 meV to the direct free exciton transition. We attribute this transition to the excited state of the direct free exciton and estimate the exciton binding energy and the Bohr radius from this separation. To do so, we need the basic parameters such as effective masses of electrons and holes and the static dielectric constant. There are a number of different values that have been reported especially for effective masses of electrons and holes and for the static dielectric constant. Taking me=10m_0 and m_h=0.8m_0 from [12] we obtain from

$$E(n) = E_g - (\mu e^4 / 2\hbar^2 \varepsilon^2 n^2) \quad (1)$$

and

$$\mu = m_e m_0 / (m_e + m_0) \quad (2)$$

a dielectric constant of 3.18 which is in good agreement with literature data ($\varepsilon = 31$ [13]). We can also estimate a Bohr radius for the free exciton of $a_B^x = 2.35$ nm and an exciton binding energy of 10 meV. In fact we have no direct correlation between crystal size and optical transitions, however, taking our value of the Bohr radius we do not expect quantum confinement effects for the particles studied in this work since their diameter exceeds the Bohr radius by a factor of 3. Comparing our data to that from the literature it is interesting to note that Monticone et al. [7], analysing the absorption edge of anatase nanoparticles, found quantum confinement effects for anatase nanoparticles only for with sizes in the range of 0.8 nm, which supports our experimental findings of the bulk behaviour of larger nanoparticles investigated in this study.

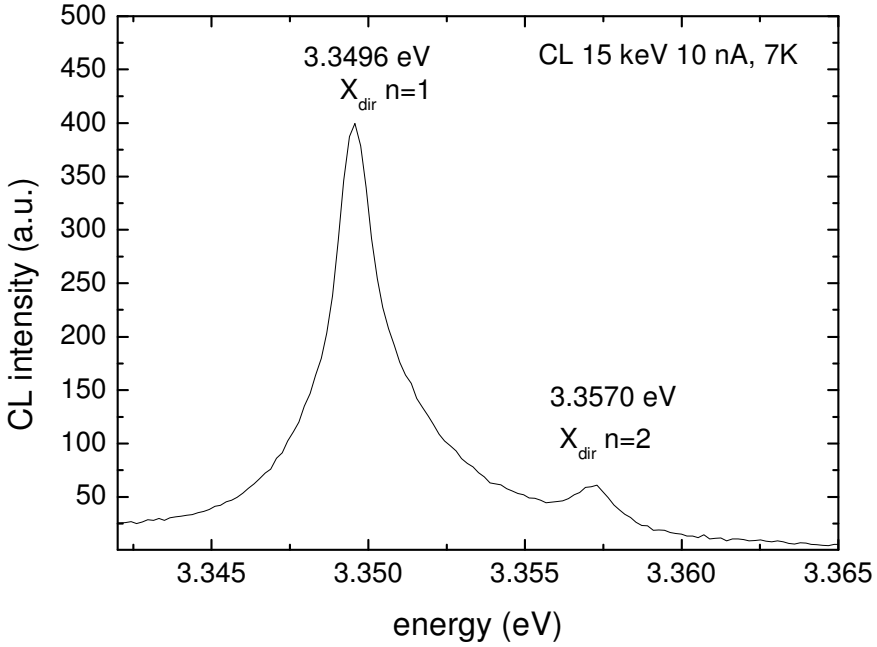

Figure 5. High resolution CL spectrum showing the ground state and the first excited state of the free excitonic transitions.

4. Conclusion

In this study we analyse optical and structural properties of anatase nanoparticles by means of HRTEM, Raman spectroscopy and CL. Cs-corrected HRTEM images show mesoporous nanoparticles with numerous defects. Additionally, small amounts of amorphous particles in the same size range as the anatase nanoparticles are being formed. The nanoparticles with an average diameter of 8.8 and 11.1 nm, respectively, show strong free exciton transitions independent of their size. From the excited state of these transitions we determine the Bohr radius of anatase transitions to be 2.35 nm. According to the best of our knowledge this the first report on free excitonic transitions in anatase TiO_2.

References

[1] Serpone N, Lawless D and Khairutdinov 1995 *J. Phys. Chem.* **99,** 16646
[2] Wunderlich W, Miao L, Tanemura M, Tanemura S, Jin P, Kaneko K, Terai A, Nabatova-Gabin N and Belkada R 2004 *Int. J. Nanosci.* **3**, 439
[3] Linsebigler AL, Lu G and Yates JT 1995 *Chem. Rev.* **95**, 735
[4] Hagfeldt A and Grätzel M 1995 *Chem. Rev.* **95**, 49
[5] Chen X and Mao SS 2007 *Chem. Rev.* **107**, 2891
[6] Bersani D, Lottici PP and Ding XZ 1998 *Appl. Phys. Lett.* **72**, 73
[7] Monticone S, Tufeu R, Kanaev AV, Scolan E and Sanchez C 2000 *Appl. Surf. Sci.* **162**, 565
[8] Kaszkur Z 2006 *Z. Kristallogr. Suppl.* **23**, 147
[9] Zhang WF, He YL, Zhang MS, Yin Z and Chen Q 2000 *J. Phys. D* **3**, 912
[10] Tang H, Berger H, Schmid PE and Lévy F 1993 *Solid State Comm.* **87**, 847
[11] Tang H, Lévy F, Berger H and Schmid PE 1995 *Phys. Rev. B* **52**, 7771
[12] Enright B and Fitzmaurice D 1996 *J. Phys. Chem.* **100,** 1027
[13] Roberts S 1949 *Phys. Rev.* **76**, 1215